Published in final edited form as:
Synapse. 2014 April ; 68(4): 131–143. doi:10.1002/syn.21723.

Anatomical and pharmacological characterization of catecholamine transients in the medial prefrontal cortex evoked by ventral tegmental area stimulation

Tatiana A. Shnitko[1] and **Donita L. Robinson**[1,2,*]

[1]Bowles Center for Alcohol Studies, University of North Carolina, Chapel Hill, NC, USA

[2]Department of Psychiatry, University of North Carolina, Chapel Hill, NC, USA

Abstract

Voltammetric measurements of catecholamines in the medial prefrontal cortex (mPFC) are infrequent because of lack of chemical selectivity between dopamine and norepinephrine and their overlapping anatomical inputs. Here, we examined the contribution of norepinephrine to the catecholamine release in the mPFC evoked by electrical stimulation of the ventral tegmental area (VTA). Initially, electrical stimulation was delivered in the midbrain at incremental depths of −5 to −9.4mm from bregma while catecholamine release was monitored in the mPFC. Although catecholamine release was observed at dorsal stimulation sites that may correspond to the dorsal noradrenergic bundle (DNB, containing noradrenergic axonal projections to the mPFC), maximal release was evoked by stimulation of the VTA (the source of dopaminergic input to the mPFC). Next, VTA-evoked catecholamine release was monitored in the mPFC before and after knife incision of the DNB, and no significant changes in the evoked catecholamine signals were found These data indicated that DNB fibers did not contribute to the VTA-evoked catecholamine release observed in the mPFC. Finally, while the D2-receptor antagonist raclopride significantly altered VTA-evoked catecholamine release, the α_2-adrenergic receptor antagonist idazoxan did not. Specifically, raclopride reduced catecholamine release in the mPFC, opposite to that observed in the striatum, indicating differential autoreceptor regulation of mesocortical and mesostriatal neurons. Together, these findings suggest that the catecholamine release in the mPFC arising from VTA stimulation was predominately dopaminergic rather than noradrenergic.

Keywords

dopamine; norepinephrine; cortex; fast-scan cyclic voltammetry; in vivo

INTRODUCTION

Many executive functions such as working memory, associative learning, selective attention and decision-making are under control of the medial prefrontal cortex (mPFC). Moreover, experimental evidence indicates that dopamine and norepinephrine in the mPFC play a

* Corresponding author: Donita L. Robinson, Bowles Center for Alcohol Studies, CB #7178, University of North Carolina, Chapel Hill, NC 27599–7178; DLR@unc.edu; Phone: 919–966–9178 ; Fax: 919–966–5679.

critical modulatory role in these cognitive functions (Robbins and Arnsten, 2009). Impairment of catecholamine (CA) neurotransmission in the mPFC has been linked to deficits in memory and attention (Lapiz and Morilak, 2006, Nelson et al., 2011), while reward and discrimination learning was accompanied by elevated CA levels in the mPFC (Mingote et al., 2004, George et al., 2011). Together, these findings support an important role of dopamine and norepinephrine activity in the mPFC and investigation of the activity of both CA in this brain area is important for understanding many cognitive functions.

Along with microdialysis, pharmacological and lesion studies, the dynamics of CA activity can be assessed in awake animals by using fast-scan cyclic voltammetry (FSCV; Robinson et al., 2008). The advantage of FSCV over other analytical techniques is that it provides high temporal and spatial resolution, and it is currently used for electrochemical detection of nanomolar concentrations of CA release in brain slices (Miles et al., 2002, Calipari et al., 2012) as well as intact brains of anaesthetized (Kuhr and Wightman, 1986, Herr et al., 2012) and awake animals (Phillips et al., 2003, Robinson et al., 2011). However, chemical selectivity is a potential problem associated with voltammetric detection. Based on the specific properties of electroactive compounds to be oxidized and reduced at different applied potentials, FSCV provides selective detection of such brain chemicals as ascorbic acid, pH and CA (Ewing et al., 1982, Runnels et al., 1999). However, this technique does not distinguish between dopamine and norepinephrine, as both CA are oxidized, and their catecholamine-*o*-quinone forms are reduced, at almost identical potentials versus an Ag/AgCl reference electrode (Kissinger et al., 1973, Park et al., 2011).

The mPFC receives dopaminergic input from the ventral tegmental area (VTA) via the medial forebrain bundle (MFB) and norepinephrine input from the locus coeruleus via the dorsal noradrenergic bundle (DNB) that merges with the MFB rostral to the VTA (Ungerstedt, 1971, Berridge and Waterhouse, 2003). CA release in the mPFC evoked by electrical stimulation of the VTA or the MFB has been measured by FSCV in anaesthetized rats (Garris et al., 1993, Lavin et al., 2005) and mice (Yavich et al., 2007) or via local stimulation in brain slices (Mundorf et al., 2001). Anatomically, dopaminergic and noradrenergic projections are overlapping in much of the MFB and electrical stimulation of this pathway would result in release of both neurotransmitters in the mPFC, while stimulation of the VTA is thought to evoke only dopamine release. However, the locus coeruleus receives dopamine projections from the VTA and stimulation of the VTA may lead to activation of the norepinephrine neurons in the locus coeruleus. For example, Deutch and colleagues observed increased norepinephrine metabolites in the PFC induced by kainic acid stimulation of the VTA, which was prevented by severing the DNB, suggesting that VTA stimulation activated locus coeruleus neurons projecting to the PFC (Deutch et al., 1986). Moreover, in rats the VTA is located close to the ventral noradrenergic bundle (VNB) that carries norepinephrine fibers to the VTA, septum and hypothalamus and eventually merges into the MFB (Ungerstedt, 1971, Johnston et al., 1987); these fibers could be antidromically activated upon electrical stimulation of the VTA. Together, these studies suggest that VTA stimulation may also activate some noradrenergic fibers, resulting in norepinephrine release simultaneously with the dopamine release in the mPFC.

The goal of the present study was to examine the relative contributions of dopamine and norepinephrine to CA release in the mPFC evoked by electrical stimulation of the VTA. We hypothesized that VTA-evoked CA release in the mPFC was primarily dopaminergic. In Experiment 1, we evaluated CA release in the mPFC evoked by midbrain electrical stimulation at progressive depths, in order to optimize the placement of electrical stimulation in the VTA. In Experiment 2, we determined the effect of severing the DNB on CA release in the mPFC evoked by electrical stimulation of the VTA. In Experiment 3, we compared CA release evoked by VTA stimulation to that evoked by more dorsal sites that may correspond to the DNB. In Experiment 4, we pharmacologically challenged the VTA-evoked CA release in the mPFC with D2 and α_2-adrenergic receptor antagonists to reveal autoreceptor modulation of the CA signal.

MATERIALS AND METHODS

Animals

Adult male Sprague-Dawley rats (N=29) were purchased from Charles River (Raleigh, NC) and housed in temperature- and humidity-controlled rooms with a 12h:12h light:dark cycle. Food and water were continuously available *ad libitum* and rats weighed 345±5 g at the time of recording. All procedures involving the animals were in accordance with the Guide for Care and Use of Laboratory Animals and were approved by the Institutional Animal Care and Use Committee of the University of North Carolina at Chapel Hill.

Surgical preparation

Rats were anesthetized with urethane (1.5g/kg, i.p.) and placed in a parallel rail stereotaxic frame (Leica Microsystems, Buffalo Grove, IL, USA) on a heated pad. The dorsal skull surface was exposed and holes were drilled in the skull for reference (Ag/AgCl), stimulating and carbon-fiber electrodes. Anterior-posterior (AP), medial-lateral (ML) and dorsal-ventral (DV) positions were referenced from bregma and all coordinates were obtained from a rat brain atlas (Paxinos and Watson, 1998). The reference electrode was placed in the left hemisphere and secured to the skull with a stainless-steel screw and dental cement. The stimulating electrode was placed above the right VTA (AP −5.2mm, ML +0.8mm, DV as noted for each experiment). In Experiment 2, an additional hole was drilled for placement of the stainless-steel surgical blade (2.75mm width, Fine Science Tools, Foster City, CA) with coordinates from bregma AP −4.2mm, ML 0 to +3mm, DV −5.0mm. The coordinates were chosen based on the CA projection mapping by Ungerstedt (1971). After the dura mater was punctured and carefully removed, the carbon-fiber microelectrode was lowered into the mPFC (AP +3.7mm, ML +2.0mm, DV −3.5mm, angle 22° toward midline). In all experiments, the position of the microelectrode remained at this implantation site during the entire recording. In Experiment 4, carbon-fiber electrodes were also placed in the caudate-putamen (CPu; AP +1.3mm, ML +1.4mm, DV −4.5mm).

Fast-scan cyclic voltammetry

Single carbon fibers (6-μm diameter) were pulled and sealed in glass capillaries. The exposed carbon fiber extended 60-120μm from the glass seal. Voltammetric recordings were made at the carbon-fiber microelectrodes every 100ms as previously described (Robinson et

al., 2005), except that the applied potential was −0.4 to +1.3V versus the Ag/AgCl reference and the scan rate was 400V/s. Voltammetric parameters, electrical stimulation parameters, and data acquisition were controlled by a computer using locally-written LabVIEW instrumentation software (National Instruments, Austin, TX, USA).

Electrical stimulation was accomplished with a bipolar, parallel, stainless-steel electrode (Ervin, 1971) insulated to the tip (0.2mm diameter for each tip; Plastics One, Roanoke, VA, USA). The tips were separated by 1.0mm. Stimulus pulses were computer-generated and were electrically isolated from the voltammetric system (NL800A Neurolog; Digitimer Ltd., UK). The electrical stimulation consisted of 24 biphasic, square-wave pulses (125μA, 2ms/phase) applied at a frequency of 60Hz.

Experimental design

Experiment 1 assessed CA release in the mPFC evoked by electrical stimulation at incremental dorsal-to-ventral positions in the midbrain in order to reveal the optimal position of the stimulating electrode to evoke CA release in the mPFC. The carbon-fiber microelectrode was positioned in the mPFC and the stimulating electrode was initially placed −5mm from bregma. CA overflow in the mPFC was monitored while the electrical stimulation was delivered, then the stimulating electrode was lowered 0.2mm, where the next stimulation was delivered. This continued until the stimulating electrode reached −9.4mm depth. In all experiments, electrical stimulations were delivered 5min apart; this time interval allowed for reproducible CA release in response to a given stimulation (Montague et al., 2004).

Experiment 2 was conducted to examine the contribution of the norepinephrine fibers in the DNB to the VTA-evoked CA release in the mPFC. At the beginning of the experiment, CA release was evoked by VTA stimulation (−8.6mm depth) and detected at the carbon-fiber electrode positioned in the mPFC; only signals with a signal-to-noise ratio of at least 5 were used. The carbon-fiber electrode was secured with dental acrylic. Next, the surgical blade was placed 1mm anterior to the stimulating electrode and lowered to 5mm below bregma. CA release was evoked by VTA stimulation every 5min and monitored in the mPFC while the blade was lowered from the initial depth of −5.0 to −9.4mm from bregma in 0.4mm increments.

Experiment 3 compared characteristics of the CA signal when evoked by stimulation at the level of the DNB versus the VTA and detected at the same recording site. With the carbon-fiber electrode positioned in the mPFC, the stimulating electrode was first placed in the DNB (−7.4mm depth, based on results from Experiment 1) and evoked CA release was measured. The stimulating electrode was then lowered to the VTA (−8.6mm depth) and the stimulation repeated.

Experiment 4 was conducted to pharmacologically modulate dopamine or norepinephrine release by applying systemic autoreceptor blockers, using the same rats as Experiment 3. Rats were separated into 3 groups (6 rats per group) that received 3mg/kg raclopride, 5mg/kg idazoxan or saline; the doses were derived from the literature (Herr et al., 2012). All injections were made intraperitoneally at volumes of 0.6ml/kg. CA release in the mPFC was

evoked every 5min with electrical stimulation of VTA (−8.6mm depth). Four electrically-evoked CA signals 5min apart were collected as a baseline measurement. Next, saline was injected in all rats as a control to provide a within-subject analysis of injection effects on release and clearance of CA in the mPFC. Four evoked CA signals were collected after saline pretreatment, and then raclopride, idazoxan or saline was injected. Electrochemical recordings of VTA-evoked CA continued for 40min following the last injection. As a positive control for Experiment 4, additional rats were used to evaluate the effect of raclopride on evoked CA overflow in the CPu. The same experimental design as described above was used except that the carbon-fiber electrode was positioned in the CPu.

Histology

At the end of each experiment, the carbon-fiber electrode placement was marked by electrical lesion made by applying continuous current (30μA for 10s) to the electrode at its recording site in the mPFC. Next, rats were cardiovascularly perfused with saline followed by 10% formalin in saline. Brains were removed and stored in 10% formalin, followed by 10% formalin/30% sucrose, then frozen and sectioned into 50-μm coronal or sagittal slices with a cryostat.

Drugs and reagents

The α2 antagonist idazoxan–HCl was obtained from Sigma-Aldrich (St. Louis, MO, USA) and the D2 antagonist raclopride was obtained from Santa Cruz Biotechnology, Inc. (Santa Cruz, CA, USA). Both drugs were dissolved in saline. Urethane was obtained from Sigma-Aldrich (St. Louis, MO, USA), dissolved in saline at concentration of 50% w/w and injected at dose of 1.5 g/kg with boosters as needed to produce a surgical plane of anesthesia.

Data analysis

Voltammetric data are presented as color plots, cyclic voltammograms, concentration-versus-time and current-versus-time traces (Michael et al., 1998). Color plots and cyclic voltammograms were used to verify the presence of CA, and the current-versus-time traces and concentration-versus-time traces were used to quantify the CA signals. Background-subtracted cyclic voltammograms were obtained by digitally subtracting voltammograms collected during baseline recording (5s immediately preceding stimulation) from those collected during and after stimulation. Temporal aspects of CA release were determined by monitoring the current at the peak oxidation potential for CA in successive voltammograms. In the traces, the peak signal amplitude ($[CA]_{max}$) and clearance half-life ($T_{1/2}$) were taken as measurements of evoked CA release and CA clearance, respectively (Yorgason et al., 2011). The signal-to-noise ratio (S:N) of the observed voltammetric signals were calculated as the signal equal to the maximal current (I_{max}) and the noise equal to the root mean square of the oxidative current in the 5s immediately before the stimulation.

As the electrochemical signals for CA and pH often overlapped during FSCV measurements (Venton et al., 2003), the contributions of each of these analytes to cyclic voltammograms were separated via principal component regression by using locally-written software (Heien et al., 2005, Keithley and Wightman, 2011). In brief, training sets of template cyclic voltammograms of electrically-evoked CA and pH (5 each) were used to identify principle

components in the voltammograms. Those components were then used to extract the relative contributions of CA and pH from the electrochemical signal in each file, yielding a concentration-versus time trace for CA (by using the *in vitro* calibration factor) and a current-versus-time trace for pH (in arbitrary units).

The electrical lesion for the verification of the electrode placements in the mPFC damaged the carbon fiber and precluded post-experimental calibration of electrode sensitivity. Thus, to estimate CA concentration from current measurements, we used the average calibration factor (μm/nA) of 86 electrodes used in previous experiments in our lab, adjusted for carbon-fiber length. Those electrodes were calibrated post-experiment, *in vitro* with a TRIS buffer containing 0, 0.5 or 1μM dopamine, as previously described (Robinson et al., 2009). Based on those electrodes, the present experiments used a calibration factor of 0.08±0.002μM CA per nA current.

Data are represented as mean ± SEM unless otherwise noted. Data were compared by using repeated-measures ANOVA or paired t-test (SigmaPlot 11.0, Systat Software, Inc., San Jose, CA, USA). If the data were not normally distributed, then they were transformed by rank before analysis or analyzed with a nonparametric test (Friedman repeated-measures ANOVA on ranks or Wilcoxon signed-rank test).

RESULTS

CA release in the mPFC evoked by midbrain electrical stimulation at progressive depths

Histological examples of electrode placements are depicted in **Supplemental Figure 1 (A, B)**. In Experiment 1, we investigated heterogeneity of CA release in the mPFC evoked by electrical stimulation delivered from −5.0 to −9.4mm DV at the midbrain area above and below the VTA (**Figure 1**) in order to optimize the site of electrical stimulation in the VTA and minimize stimulation of the DNB in the following experiments. The carbon-fiber electrode was placed to the mPFC and remained at this site during the entire recording, while the stimulating electrode was placed above the right VTA (−5.0 mm bellow bregma) and lowered every 5 min with the inclement 0.2 mm followed by electrical stimulation. Based on previous studies and atlases (Park et al., 2009, Paxinos et al., 2009), we expected any CA release due to the DNB to be observed at depths of −5.5 to −7.5mm, while release due to VTA stimulation would occur below −8.0mm. Representative current versus time traces with corresponding background-subtracted cyclic voltammograms recorded in the mPFC of an individual rat at the various stimulation depths are shown in **Figure 1A**. When electrical stimulation was made at −5.0mm below bregma, neither the current trace nor the corresponding voltammograms indicated CA release. At −5.8mm, electrical stimulation produced the first detectable changes in voltammetric current in this rat, and the cyclic voltammogram from the peak of the signal established that this change in current was due to CA release. The maximum increase in the observed voltammetric current in this rat was observed when stimulation was delivered at −8.6mm, also confirmed to be due to oxidation of CA by the cyclic voltammogram.

A schematic illustration of the track of electrical stimulation through the midbrain is presented in **Figure 1B**. Two regions potentially capable to provide CA release in the mPFC

were the DNB for norepinephrine and the VTA for dopamine. For each rat, we obtained the pattern of CA release in the mPFC evoked by electrical stimulation at progressive depths. Next, the peak current of the evoked CA signals at various depths (I_d) were normalized to the maximal response (I_d^{max}) observed in each rat. In **Figure 1C**, the normalized signals recorded in the mPFC (n=5 rats) are shown as a function of stimulation depth. Electrically-evoked CA responses observed in the mPFC progressively increased with lower stimulations from −5.0mm (18±7% of I_d^{max}) to −7.4mm (61±10% of I_d^{max}), although the increased oxidative current was not significantly different from baseline (i.e., signals at depth −5.0 mm). Across rats, the I_d^{max} detected in the mPFC was observed at depths from −8.4 to −9.0 mm from bregma, and the group-average I_d^{max} was evoked by electrical stimulation at −8.4 to −8.6mm, corresponding to the VTA (Paxinos et al., 2009). The average VTA-evoked CA response detected in the mPFC was 1.9±0.8nA at −8.4mm and 1.9±0.7nA at −8.6mm. Friedman repeated-measures ANOVA on ranks of I_d by stimulation depth revealed a significant effect of depth (χ^2_{21}=65.9, p<0.001), and posthoc comparison confirmed that only stimulation of the VTA (depths −8.4 to −9.0mm) yielded significantly larger I_d versus −5.0mm (Dunnett's method of multiple comparisons versus control depth, all q'>3.1, all p<0.05).

It was possible that electrical stimulation at depths near the DNB were releasing norepinephrine in the mPFC, but the carbon-fiber microelectrodes were insensitive to norepinephrine. To test this we calibrated 8 additional electrodes *in vitro* for both norepinephrine and dopamine. The electrodes detected both neurotransmitters, but were twice as sensitive to dopamine versus norepinephrine; the signal for 1μM NE was 7.7±1.6nA and for 1μM DA was 13.9±2.1nA (paired t-test, t_7=5.2, p<0.01).

Effect of DNB knife cut on CA release in the mPFC evoked by VTA stimulation

In Experiment 2, we examined the contribution of norepinephrine to mPFC CA release evoked by electrical stimulation of the VTA. We hypothesized that if norepinephrine contributed to the mPFC signal, then severing DNB fibers would decrease VTA-stimulated release. To test this, we detected VTA-evoked CA release in the mPFC and then situated a surgical blade at 5.0mm below bregma, 1mm anterior to the stimulating electrode (AP: −4.2 mm from bregma). Next, the blade was lowered in 0.4mm increments while the stimulating electrode was fixed in the VTA and evoked CA release was monitored in the mPFC. A histological example of the knife placed ~1 mm anterior from the stimulating electrode is depicted in **Supplemental Figure 1C**.

Representative current-versus-time traces and corresponding background-subtracted CVs recorded in the mPFC of an individual rat are shown in **Figure 2A** and group data are shown in **Figure 2C** (n=4 rats). The track of the surgical blade through the midbrain (slightly anterior to **Figure 1B**) is schematically presented in **Figure 2B**, indicating the approximate placement of the DNB (norepinephrine fibers) and MFB (dopamine fibers). We normalized VTA-evoked CA signals (I_d) for each rat by dividing by the observed response at knife-depth −5.0 mm (I_{-5mm}) observed in each rat. The average current detected in the mPFC and evoked by stimulation of the VTA was 0.8±0.2nA when the knife was −5.0mm and 0.9±0.2nA at −7.4mm below bregma. The evoked CA signal decreased only after the knife

reached −8.6mm (0.6±0.2nA), and continued to decrease until the knife reached −9.4mm (0.4±0.2nA). A 1-way repeated-measures ANOVA of I_d by knife depth (calculated on the raw data) revealed a significant effect of depth ($F_{11,29}$=4.2, p<0.001), and posthoc comparison confirmed that only knife cuts of the MFB at −9.4mm below bregma significantly reduced I_d versus the signal at −5.0mm (Bonferroni t-test, t=4.3, p<0.05). When considering individual recordings, 3 of the 4 rats exhibited progressive reduction of CA signals by 60±21% and 74±6% of current recorded at −5.0 mm after knife cut at depth −9.0 and −9.4 mm, respectively. In the remaining rat, the knife cut reduced CA release at depths of −9.0 and −9.4 by 15% and 30%, but did not eliminate it.

Dynamics of CA release and clearance in mPFC evoked by electrical stimulation of the DNB and VTA

Experiment 3 compared CA signals in the mPFC evoked by stimulation at DNB versus VTA depths (n=18 rats). Initial CA release was evoked by electrical stimulation of the DNB (−7.4mm depth), and then the stimulating electrode was lowered to the VTA (−8.6mm depth); DNB and VTA stimulation sites were chosen based on results from Experiment 1. The S:N of the CA oxidative current in the mPFC evoked by VTA stimulation was 4-fold higher than that evoked by DNB stimulation (28.8±4.7 versus 7.6±2.2, respectively); this difference was significant via a Wilcoxon signed-rank test (Z=3.7, p<0.001).

We next compared measures of CA release ($[CA]_{max}$) and clearance ($T_{1/2}$) in signals evoked by DNB versus VTA stimulation. In order to confidently measure $[CA]_{max}$ and $T_{1/2}$, we restricted the analysis to rats that yielded S:N ratios >5 at both stimulation sites. (An example of a voltammetric signal with a S:N ratio of 5.1 is shown in **Supplemental Figure 2**.) The S:N ratio of VTA-evoked CA release was >5 in all rats, while the ratio of DNB-evoked CA release was >5 in only 7 rats. We found that electrical stimulation of the DNB did not evoke sufficient (S:N>5) CA release in the mPFC of 11 rats and averaged peak current observed in these animals was 1.6-fold smaller (0.53±0.13 nA) than in rats with S:N>5.0 (0.93±0.13 nA). **Figure 3** shows examples of CA release and clearance in the mPFC evoked by stimulation of the DNB or VTA (−7.4 or −8.6mm from bregma, respectively). CA signals in the mPFC evoked by electrical stimulation at −7.4 and −8.6mm in the same rat are shown in **Figure 3A**. The color plots (Michael et al., 1998) display current (color) at applied potentials (y-axis) over time (x-axis). Overlaid on the color plot is the concentration versus time trace at 0.65V (the peak oxidation potential of CA), with the dotted lines indicating where $[CA]_{max}$ and $T_{1/2}$ are measured; the electrochemical data were analyzed with principal component regression before determination of $[CA]_{max}$ and $T_{1/2}$. In this rat, $[CA]_{max}$ was reduced while $T_{1/2}$ was similar when evoked by stimulation of the DNB versus the VTA. **Figure 3B** displays composite data across the 7 rats with sufficient S:N in both stimulation sites. CA release was significantly lower after DNB stimulation than after VTA stimulation ($[CA]_{max}$: paired *t*-test, t_6=−4.97, p<0.005). In contrast, there was no difference in CA clearance between the two stimulation sites ($T_{1/2}$: paired *t*-test, t_6=0.65, p>0.05).

Effect of autoreceptor antagonists on CA release and uptake in the mPFC

Next, in order to further investigate the contributions of dopamine and norepinephrine to the observed voltammetric signals, Experiment 4 examined the effects of D2- and α2-adrenergic receptor antagonists (raclopride and idazoxan, respectively) on VTA-evoked CA release and clearance in the mPFC. We hypothesized that if there was no contribution of norepinephrine to the CA release evoked by VTA stimulation delivered at depth −8.6 mm from bregma, then inhibition of α_2-adrenergic autoreceptors should not alter the signals. In the 18 rats from Experiment 3, VTA-evoked CA release was monitored at baseline, after saline and after drug injection (saline, raclopride or idazoxan); the saline pretreatment allowed within-subject analysis of drug effects.

Representative effects of the antagonists on VTA-evoked voltammetric signals observed in individual rats are shown in **Figure 4A**. Color plots demonstrate that administration of idazoxan had no effect on VTA-evoked CA release whereas injection of raclopride decreased mPFC CA release. In addition, concentration-versus-time traces (**Figure 4B**, averaged across rats per group) demonstrate slightly decreased evoked CA release in 20 and 40 min after raclopride but not idazoxan injection.

Figure 5A shows the group effects of raclopride, idazoxan and saline on $[CA]_{max}$ in the mPFC over time. The baseline and saline time points were averaged for clarity (4 evoked signals each). Saline and idazoxan did not significantly alter $[CA]_{max}$. In contrast, raclopride significantly decreased $[CA]_{max}$ by 26% from baseline and 20% from saline pretreatment within 20min after injection. A 2-way repeated-measures ANOVA yielded a significant group-by-time interaction ($F_{6,45}$=4.3, $p<0.005$) with no significant main effects. Posthoc comparisons showed that $[CA]_{max}$ in the raclopride group was significantly reduced at 20 and 40min versus baseline and at 20min versus saline (Bonferroni t-test, all $t>2.9$, all $p<0.05$), but not versus idazoxan (all $p>0.3$). $[CA]_{max}$ in the saline and idazoxan groups did not change.

The autoreceptor antagonists did not significantly alter CA clearance in the mPFC as measured by $T_{1/2}$ versus the saline group (**Figure 5B**). Across all groups, $T_{1/2}$ slightly increased over time, indicating slower clearance, although there was variability across rats, especially in the idazoxan group. A 2-way repeated-measures ANOVA on $T_{1/2}$ (transformed by rank) yielded a significant main effect of time ($F_{6,45}$=2.9, $p<0.05$), but no significant effects of group or group by time interaction ($p>0.05$). However, no individual timepoints were significantly different from another after Bonferonni correction (all $t<2.7$, $p>0.05$). To verify that we were not simply underpowered to detect a reliable effect of idaxozan on $T_{1/2}$, we calculated the number of rats required to detect a difference: for power = 0.8 and population parameters equal to those found in this data set, 59 rats would be required to reach statistical significance, confirming the heterogeneity of $T_{1/2}$ in response to idaxozan.

Previous studies have shown that D2 receptor antagonists potentiate dopamine release evoked by MFB stimulation and monitored in the dorsal striatum (Yavich, 1996, Benoit-Marand et al., 2001, Wu et al., 2002). Therefore, as a positive control to the raclopride-induced decrease of evoked CA release observed in the mPFC, we examined effect of raclopride on evoked dopamine release in the CPu (**Supplemental Figure 3**). The color

plots and concentration-versus-time traces demonstrate that dopamine release in the CPu evoked by VTA stimulation was 3-fold larger than CA release in the mPFC. Moreover, raclopride robustly increased dopamine release in the CPu (n = 2 rats), consistent with previous studies.

DISCUSSION

While FSCV is the method of choice to evaluate dopamine release and clearance kinetics *in vivo* and in real time, its application to cortical dopamine dynamics has been limited by the ability of FSCV to distinguish dopamine from norepinephrine inputs. Thus, this study aimed to investigate relative contributions of dopamine and norepinephrine to VTA-evoked CA release measured in the mPFC of anesthetized rats. We found that electrical stimulation of either the DNB or the VTA produced CA release in the mPFC. Furthermore, VTA-evoked CA release was unaffected by a knife cut through the DNB, suggesting that ascending norepinephrine fibers did not contribute to that mPFC electrochemical signal. Additional confirmation that the VTA-evoked CA signal was primarily dopaminergic was that a D2 receptor antagonist, but not an α_2-adrenergic receptor antagonist, reliably altered $[CA]_{max}$. Together, these data provide anatomical and pharmacological evidence that VTA-evoked CA release in the mPFC is primarily dopaminergic, validating this method for future measurements of dopamine release and uptake kinetics in animal models of neuropharmacology and psychiatric disease. Indeed, this initial study revealed differential effects of D2-autoreceptor regulation on dopamine release in the mPFC as compared to striatum.

The key challenge of the current study was to differentiate dopamine from norepinephrine input to the mPFC via selective electrical stimulation of dopamine neurons. While carbon-fiber electrodes are less sensitive to norepinephrine than to dopamine (e.g., the present study; Heien et al., 2003, Robinson et al., 2003, Noga et al., 2004), this fact does not exclude the possibility that norepinephrine might contribute to the CA signals measured in the mPFC and evoked by electrical stimulation in the midbrain. Axons from the norepinephrine neurons of A1, A2, A5, A6 and A7 cell groups form the ascending noradrenergic bundle, which separates into the DNB and VNB. The DNB carries norepinephrine fibers to the thalamus, hypothalamus and cortex, including the mPFC (Ungerstedt, 1971). During FSCV measurements of norepinephrine in the anteroventral thalamic nucleus (a target of norepinephrine axons in the DNB), maximal release was evoked by midbrain electrical stimulation of −5.5 to −7.0mm depth that presumably activated the DNB (Park et al., 2009). With a more medial stimulation track than used by Park and colleagues (0.8 versus 1.2mm lateral), we found two local maxima of CA release upon electrical stimulation of the midbrain: at −7.4mm and −8.4/−8.6mm below bregma. This spacing is consistent with histological depictions of the DNB versus the VTA; for example, tyrosine hydroxlase-positive fibers in the DNB (shown as the dorsal tegmental tract) are located 1.0-1.5mm above the tyrosine hydroxlase-positive soma and fibers of the VTA and substantia nigra (Figure 248 in (Paxinos et al., 2009). Thus, we conclude that electrical stimulation at −7.4mm below bregma in the present experiment activates the DNB and the resulting CA release is likely to arise predominantly from norepinephrine terminals in the mPFC.

Although the VTA is spatially distinct from the DNB and the norepinephrine fibers directly innervating the mPFC, VTA stimulation could conceivably activate the locus coeruleus and, thus, indirectly activate mPFC-projecting norepinephrine neurons. Specifically, electrical stimulation of the VTA would activate the VTA projection to the locus coeruleus and may antidromically activate fibers in the adjacent VNB that arise from the locus coeruleus. Thus, we assessed the potential contribution of norepinephrine to the VTA-evoked dopamine signal in the mPFC by severing the DNB and found that $[CA]_{max}$ was unchanged by a knife lowered from −5.0 to −8.2mm below bregma, which would include the DNB. In fact, a decrease in $[CA]_{max}$ was not detected until −8.6mm or lower, at the level of the MFB. Therefore, our data indicate that norepinephrine fibers in the DNB do not contribute to the transient CA release evoked by VTA stimulation, consistent with previous recordings in the mPFC in which very similar $[CA]_{max}$ was evoked by VTA/substantia nigra stimulation and by MFB stimulation (Garris et al., 1993, Garris and Wightman, 1994). Nonetheless, VTA activity may tonically regulate norepinephrine transmission. Indeed, Deutch et al. (1986) observed increased norepinephrine metabolites in the mPFC and hippocampus induced by kainic acid in the VTA that was blocked by a knife cut of the DNB, suggesting that VTA neurons regulate activity of norepinephrine projections that travel in the DNB (Deutch et al., 1986). As DNB fibers did not contribute to the immediate CA transient evoked by VTA stimulation in the present study, we suggest that the VTA regulation of norepinephrine projections occurs on a slower timescale than is assessed with FSCV.

When comparing CA release in the mPFC evoked by midbrain stimulation at the level of the DNB versus the VTA, we found that both sites elicited CA release but $[CA]_{max}$ was significantly larger at VTA stimulation. Considering that the mPFC contains more norepinephrine than dopamine (Garris et al., 1993), this discrepancy may be due to more optimal placement of the stimulating electrode to activate dopamine fibers as opposed to norepinephrine fibers, in addition to enhanced sensitivity to dopamine versus norepinephrine under the current electrochemical conditions. Indeed, the present study aimed to minimize DNB stimulation by medial placement of the stimulating electrode. The finding that CA clearance rates were similar after both stimulation sites was not unexpected, as both norepinephrine and dopamine are cleared by identical mechanisms in the mPFC, including uptake by the norepinephrine transporter and metabolism by catechol-*O*-methyltransferase and monoamine oxidase (Kaenmaki et al., 2010). Garris et al. (1993) also examined CA release in the mPFC evoked by midbrain stimulation, lowering the stimulating electrode in a ventral path. They reported that the first observable increase in $[CA]_{max}$ occurred at a stimulation depth of −7.5mm below dura and the peak response was observed at −8.5mm, similar to the present findings. In contrast to the present study, the previous work did not detect CA release at more dorsal stimulation sites (Garris et al., 1993, Garris and Wightman, 1994), but this discrepancy is likely due to the enhanced sensitivity of the FSCV parameters currently in use (Robinson and Wightman, 2007).

It is known that dopamine has higher affinity to NET than norepinephrine does (Raiteri et al., 1977), and in the PFC both NET on norepinephrine terminals (Carboni et al., 1990, Yamamoto and Novotney, 1998) and COMT (Kaenmaki et al., 2010) play important roles in dopamine decay from the extracellular fluid. Thus, administration of DAT or NET blockers

would not selectively alter DA and NE concentrations, respectively, in the PFC. Instead, to pharmacologically confirm the dopaminergic nature of VTA-evoked CA release in the mPFC, we systemically administered either a D2 or α_2-adrenergic receptor antagonist, as D2 autoreceptors regulate dopamine release (Gonon and Buda, 1985, Wu et al., 2002), while α_2-adrenergic autoreceptors regulate norepinephrine release (Devoto et al., 2004). We hypothesized that if VTA stimulation evoked primarily dopamine release in the mPFC, then the release should be altered by administration of D2 but not α_2-adrenergic receptor antagonists. Supporting this hypothesis, idazoxan did not significantly alter VTA-evoked CA release or clearance in the mPFC, although the same dose increased norepinephrine release and clearance in the bed nucleus of the stria terminalis (Herr et al., 2012). In contrast, raclopride reliably reduced $[CA]_{max}$, consistent with the sensitivity of VTA-evoked CA release to dopamine autoreceptor regulation, although the conclusions made here are moderated by the fact that the effects of raclopride were not significantly different from idazoxan. The time course of systemic activity of the two antagonists should be considered in this study. Based on literature, both drugs are effective within the time frame of the current study after intraperitoneal injections. Thus, previous studies demonstrated that 2mg/kg raclopride increases dopamine concentrations as measured by microdialysis within 40min after injection (See et al., 1991) and within 30min as measured with FSCV (Park et al., 2010). In our study we used raclopride at a higher dose (3mg/kg) and observed its effect within 20min after injection. Similarly, FSCV studies demonstrated that 5mg/kg idazoxan increased norepinephrine release in the bed nucleus of the stria terminalis in 20min after injection (Herr et al., 2012, Park et al., 2012).

The effect of raclopride on $[CA]_{max}$ in the mPFC was opposite to what the present study and others have observed on dopamine release in the CPu (Wu et al., 2002, Park et al., 2010). Striatal dopamine release is regulated by autoreceptor feedback, including impulse modulation via activation of D2 receptors on dopamine soma and synthesis modulation via activation of receptors on dopamine terminals. However, autoreceptor regulation of dopamine release in mesocortical neurons is less characterized. In the mouse VTA, Lammel and colleagues found a lack of somatodendritic D2 autoreceptors on the PFC-projecting neurons, as well as projection-specific differences in tyrosine hydroxylase, dopamine transporter and vesicular monoamine transporter 2 expression (Lammel et al., 2008). However, rat mesocortical neurons evidently express somatic D2 autoreceptors, as Margolis and colleagues determined that the D2 agonist quinpirole induced hyperpolarization of VTA neurons projecting to the PFC (Margolis et al., 2008). The difference in autoreceptor regulation of VTA-evoked CA/dopamine release between striatum and mPFC might be due to differential expression of autoreceptors on the soma versus the terminals, a possibility that can be tested by using FSCV with local infusion of D2 receptor ligands.

In conclusion, this study provides anatomical and pharmacological evidence that VTA-evoked CA release in the mPFC is predominantly dopaminergic, validating an additional tool to investigate mesocortical dopamine release and clearance in animal models of development and disease. The data additionally revealed autoreceptor regulation of mPFC dopamine release that differs from that in striatal regions and that likely contributes to differential dopamine transmission across terminal regions. Future studies could characterize norepinephrine release in the mPFC by targeting the DNB with more lateral stimulation sites

and investigating the effects of similar anatomical and pharmacological manipulations on DNB-evoked CA release.

Supplementary Material

Refer to Web version on PubMed Central for supplementary material.

Acknowledgments

The authors thank Katherine Joa and Laura Kennerly for excellent technical assistance and Dr. Zoe McElligott for critical comments on the manuscript. This research was funded by the National Institute of Alcoholism and Alcohol Abuse (R01-AA018008, U01-AA019972) and the UNC Bowles Center for Alcohol Studies.

Abbreviations

AP	anterior-posterior
CA	catecholamine
$[CA]_{max}$	maximum concentration of catecholamine
CPu	caudate putamen
DNB	dorsal noradrenergic bundle
DV	dorsal-ventral
FSCV	fast scan cyclic voltammetry
I_d	current at stimulation depth
I_d^{max}	maximum current detected across stimulation depths
I_{max}	maximum current
ML	medial-lateral
mPFC	medial prefrontal cortex
S:N	signal-to-noise ratio
$T_{1/2}$	time to clear half of $[CA]_{max}$
VNB	ventral noradrenergic bundle
VTA	ventral tegmental area

REFERENCES

Benoit-Marand M, Borrelli E, Gonon F. Inhibition of dopamine release via presynaptic D2 receptors: time course and functional characteristics in vivo. J Neurosci. 2001; 21:9134–9141. [PubMed: 11717346]

Berridge CW, Waterhouse BD. The locus coeruleus-noradrenergic system: modulation of behavioral state and state-dependent cognitive processes. Brain Res Brain Res Rev. 2003; 42:33–84. [PubMed: 12668290]

Calipari ES, Huggins KN, Mathews TA, Jones SR. Conserved dorsal-ventral gradient of dopamine release and uptake rate in mice, rats and rhesus macaques. Neurochem Int. 2012

Carboni E, Tanda GL, Frau R, Di Chiara G. Blockade of the noradrenaline carrier increases extracellular dopamine concentrations in the prefrontal cortex: evidence that dopamine is taken up in vivo by noradrenergic terminals. J Neurochem. 1990; 55:1067–1070. [PubMed: 2117046]

Deutch AY, Goldstein M, Roth RH. Activation of the locus coeruleus induced by selective stimulation of the ventral tegmental area. Brain Res. 1986; 363:307–314. [PubMed: 3942901]

Devoto P, Flore G, Pira L, Longu G, Gessa GL. Alpha2-adrenoceptor mediated co-release of dopamine and noradrenaline from noradrenergic neurons in the cerebral cortex. J Neurochem. 2004; 88:1003–1009. [PubMed: 14756822]

Ervin, FR. Electrical stimulation of the brain.. In: Myers, RD., editor. Methods in psychobiology Laboratory techniques in neuropsychology and neurobiology. Vol. 1. Acadenic Press Inc.; London and New York: 1971. p. 356

Ewing AG, Wightman RM, Dayton MA. In vivo voltammetry with electrodes that discriminate between dopamine and ascorbate. Brain Res. 1982; 249:361–370. [PubMed: 6814706]

Garris PA, Collins LB, Jones SR, Wightman RM. Evoked extracellular dopamine in vivo in the medial prefrontal cortex. J Neurochem. 1993; 61:637–647. [PubMed: 8336146]

Garris PA, Wightman RM. Different kinetics govern dopaminergic transmission in the amygdala, prefrontal cortex, and striatum: an in vivo voltammetric study. J Neurosci. 1994; 14:442–450. [PubMed: 8283249]

George DN, Jenkins TA, Killcross S. Dissociation of prefrontal cortex and nucleus accumbens dopaminergic systems in conditional learning in rats. Behav Brain Res. 2011; 225:47–55. [PubMed: 21741412]

Gonon FG, Buda MJ. Regulation of dopamine release by impulse flow and by autoreceptors as studied by in vivo voltammetry in the rat striatum. Neuroscience. 1985; 14:765–774. [PubMed: 2986044]

Heien ML, Khan AS, Ariansen JL, Cheer JF, Phillips PE, Wassum KM, Wightman RM. Real-time measurement of dopamine fluctuations after cocaine in the brain of behaving rats. Proceedings of the National Academy of Sciences of the United States of America. 2005; 102:10023–10028. [PubMed: 16006505]

Heien ML, Phillips PE, Stuber GD, Seipel AT, Wightman RM. Overoxidation of carbon-fiber microelectrodes enhances dopamine adsorption and increases sensitivity. Analyst. 2003; 128:1413–1419. [PubMed: 14737224]

Herr NR, Park J, McElligott ZA, Belle AM, Carelli RM, Wightman RM. In vivo voltammetry monitoring of electrically evoked extracellular norepinephrine in subregions of the bed nucleus of the stria terminalis. J Neurophysiol. 2012; 107:1731–1737. [PubMed: 22190618]

Johnston CA, Mattiace LA, Negro-Vilar A. Effect of ventral noradrenergic bundle lesions on concentrations of monoamine neurotransmitters and metabolites in several discrete areas of the rat brain. Cell Mol Neurobiol. 1987; 7:403–411. [PubMed: 2454160]

Kaenmaki M, Tammimaki A, Myohanen T, Pakarinen K, Amberg C, Karayiorgou M, Gogos JA, Mannisto PT. Quantitative role of COMT in dopamine clearance in the prefrontal cortex of freely moving mice. J Neurochem. 2010; 114:1745–1755. [PubMed: 20626558]

Keithley RB, Wightman RM. Assessing principal component regression prediction of neurochemicals detected with fast-scan cyclic voltammetry. ACS Chem Neurosci. 2011; 2:514–525. [PubMed: 21966586]

Kissinger PT, Hart JB, Adams RN. Voltammetry in brain tissue--a new neurophysiological measurement. Brain Res. 1973; 55:209–213. [PubMed: 4145914]

Kuhr WG, Wightman RM. Real-time measurement of dopamine release in rat brain. Brain Res. 1986; 381:168–171. [PubMed: 3489505]

Lammel A, Schwab M, Slotta U, Winter G, Scheibel T. Processing conditions for the formation of spider silk microspheres. ChemSusChem. 2008; 1:413–416. [PubMed: 18702135]

Lapiz MD, Morilak DA. Noradrenergic modulation of cognitive function in rat medial prefrontal cortex as measured by attentional set shifting capability. Neuroscience. 2006; 137:1039–1049. [PubMed: 16298081]

Lavin A, Nogueira L, Lapish CC, Wightman RM, Phillips PE, Seamans JK. Mesocortical dopamine neurons operate in distinct temporal domains using multimodal signaling. J Neurosci. 2005; 25:5013–5023. [PubMed: 15901782]

Margolis EB, Mitchell JM, Ishikawa J, Hjelmstad GO, Fields HL. Midbrain dopamine neurons: projection target determines action potential duration and dopamine D(2) receptor inhibition. J Neurosci. 2008; 28:8908–8913. [PubMed: 18768684]

Michael D, Travis ER, Wightman RM. Color images for fast-scan CV measurements in biological systems. Anal Chem. 1998; 70:586A–592A.

Miles PR, Mundorf ML, Wightman RM. Release and uptake of catecholamines in the bed nucleus of the stria terminalis measured in the mouse brain slice. Synapse. 2002; 44:188–197. [PubMed: 11954051]

Mingote S, de Bruin JP, Feenstra MG. Noradrenaline and dopamine efflux in the prefrontal cortex in relation to appetitive classical conditioning. J Neurosci. 2004; 24:2475–2480. [PubMed: 15014123]

Montague PR, McClure SM, Baldwin PR, Phillips PE, Budygin EA, Stuber GD, Kilpatrick MR, Wightman RM. Dynamic gain control of dopamine delivery in freely moving animals. J Neurosci. 2004; 24:1754–1759. [PubMed: 14973252]

Mundorf ML, Joseph JD, Austin CM, Caron MG, Wightman RM. Catecholamine release and uptake in the mouse prefrontal cortex. J Neurochem. 2001; 79:130–142. [PubMed: 11595765]

Nelson AJ, Cooper MT, Thur KE, Marsden CA, Cassaday HJ. The effect of catecholaminergic depletion within the prelimbic and infralimbic medial prefrontal cortex on recognition memory for recency, location, and objects. Behav Neurosci. 2011; 125:396–403. [PubMed: 21480692]

Noga BR, Pinzon A, Mesigil RP, Hentall ID. Steady-state levels of monoamines in the rat lumbar spinal cord: spatial mapping and the effect of acute spinal cord injury. J Neurophysiol. 2004; 92:567–577. [PubMed: 15014108]

Park J, Aragona BJ, Kile BM, Carelli RM, Wightman RM. In vivo voltammetric monitoring of catecholamine release in subterritories of the nucleus accumbens shell. Neuroscience. 2010; 169:132–142. [PubMed: 20451589]

Park J, Kile BM, Wightman RM. In vivo voltammetric monitoring of norepinephrine release in the rat ventral bed nucleus of the stria terminalis and anteroventral thalamic nucleus. Eur J Neurosci. 2009; 30:2121–2133. [PubMed: 20128849]

Park J, Takmakov P, Wightman RM. In vivo comparison of norepinephrine and dopamine release in rat brain by simultaneous measurements with fast-scan cyclic voltammetry. J Neurochem. 2011; 119:932–944. [PubMed: 21933188]

Park J, Wheeler RA, Fontillas K, Keithley RB, Carelli RM, Wightman RM. Catecholamines in the bed nucleus of the stria terminalis reciprocally respond to reward and aversion. Biol Psychiatry. 2012; 71:327–334. [PubMed: 22115620]

Paxinos, G.; Watson, C., editors. The rat brain in stereotaxic coordinates. Academic Press; 1998.

Paxinos, G.; Watson, C.; Carrive, P.; Kirkcaldie, M.; Ashwell, KW., editors. Chemoarchitectonic atlas of the rat brain. Academic Press; 2009.

Phillips PE, Stuber GD, Heien ML, Wightman RM, Carelli RM. Subsecond dopamine release promotes cocaine seeking. Nature. 2003; 422:614–618. [PubMed: 12687000]

Raiteri M, Del Carmine R, Bertollini A, Levi G. Effect of sympathomimetic amines on the synaptosomal transport of noradrenaline, dopamine and 5-hydroxytryptamine. Eur J Pharmacol. 1977; 41:133–143. [PubMed: 832672]

Robbins TW, Arnsten AF. The neuropsychopharmacology of fronto-executive function: monoaminergic modulation. Annu Rev Neurosci. 2009; 32:267–287. [PubMed: 19555290]

Robinson DL, Hermans A, Seipel AT, Wightman RM. Monitoring Rapid Chemical Communication in the Brain. Chemical reviews. 2008; 108:2554–2584. [PubMed: 18576692]

Robinson DL, Howard EC, McConnell S, Gonzales RA, Wightman RM. Disparity between tonic and phasic ethanol-induced dopamine increases in the nucleus accumbens of rats. Alcoholism, clinical and experimental research. 2009; 33:1187–1196.

Robinson DL, Venton BJ, Heien ML, Wightman RM. Detecting subsecond dopamine release with fast-scan cyclic voltammetry in vivo. Clin Chem. 2003; 49:1763–1773. [PubMed: 14500617]

Robinson DL, Volz TJ, Schenk JO, Wightman RM. Acute ethanol decreases dopamine transporter velocity in rat striatum: in vivo and in vitro electrochemical measurements. Alcoholism, clinical and experimental research. 2005; 29:746–755.

Robinson, DL.; Wightman, RM. Rapid Dopamine Release in Freely Moving Rats.. In: Michael, AC.; Borland, LM., editors. Electrochemical Methods for Neuroscience. CRC Press; Boca Raton: 2007. p. 17-34.

Robinson DL, Zitzman DL, Williams SK. Mesolimbic dopamine transients in motivated behaviors: focus on maternal behavior. Front Psychiatry. 2011; 2:23. [PubMed: 21629844]

Runnels PL, Joseph JD, Logman MJ, Wightman RM. Effect of pH and surface functionalities on the cyclic voltammetric responses of carbon-fiber microelectrodes. Anal Chem. 1999; 71:2782–2789. [PubMed: 10424168]

See RE, Sorg BA, Chapman MA, Kalivas PW. In vivo assessment of release and metabolism of dopamine in the ventrolateral striatum of awake rats following administration of dopamine D1 and D2 receptor agonists and antagonists. Neuropharmacology. 1991; 30:1269–1274. [PubMed: 1686300]

Ungerstedt U. Stereotaxic mapping of the monoamine pathways in the rat brain. Acta Physiol Scand Suppl. 1971; 367:1–48. [PubMed: 4109331]

Venton BJ, Michael DJ, Wightman RM. Correlation of local changes in extracellular oxygen and pH that accompany dopaminergic terminal activity in the rat caudate-putamen. JNeurochem. 2003; 84:373–381. [PubMed: 12558999]

Wu Q, Reith ME, Walker QD, Kuhn CM, Carroll FI, Garris PA. Concurrent autoreceptor-mediated control of dopamine release and uptake during neurotransmission: an in vivo voltammetric study. J Neurosci. 2002; 22:6272–6281. [PubMed: 12122086]

Yamamoto BK, Novotney S. Regulation of extracellular dopamine by the norepinephrine transporter. J Neurochem. 1998; 71:274–280. [PubMed: 9648875]

Yavich L. Two simultaneously working storage pools of dopamine in mouse caudate and nucleus accumbens. Br J Pharmacol. 1996; 119:869–876. [PubMed: 8922734]

Yavich L, Forsberg MM, Karayiorgou M, Gogos JA, Mannisto PT. Site-specific role of catechol-O-methyltransferase in dopamine overflow within prefrontal cortex and dorsal striatum. J Neurosci. 2007; 27:10196–10209. [PubMed: 17881525]

Yorgason JT, Espana RA, Jones SR. Demon voltammetry and analysis software: analysis of cocaine-induced alterations in dopamine signaling using multiple kinetic measures. J Neurosci Methods. 2011; 202:158–164. [PubMed: 21392532]

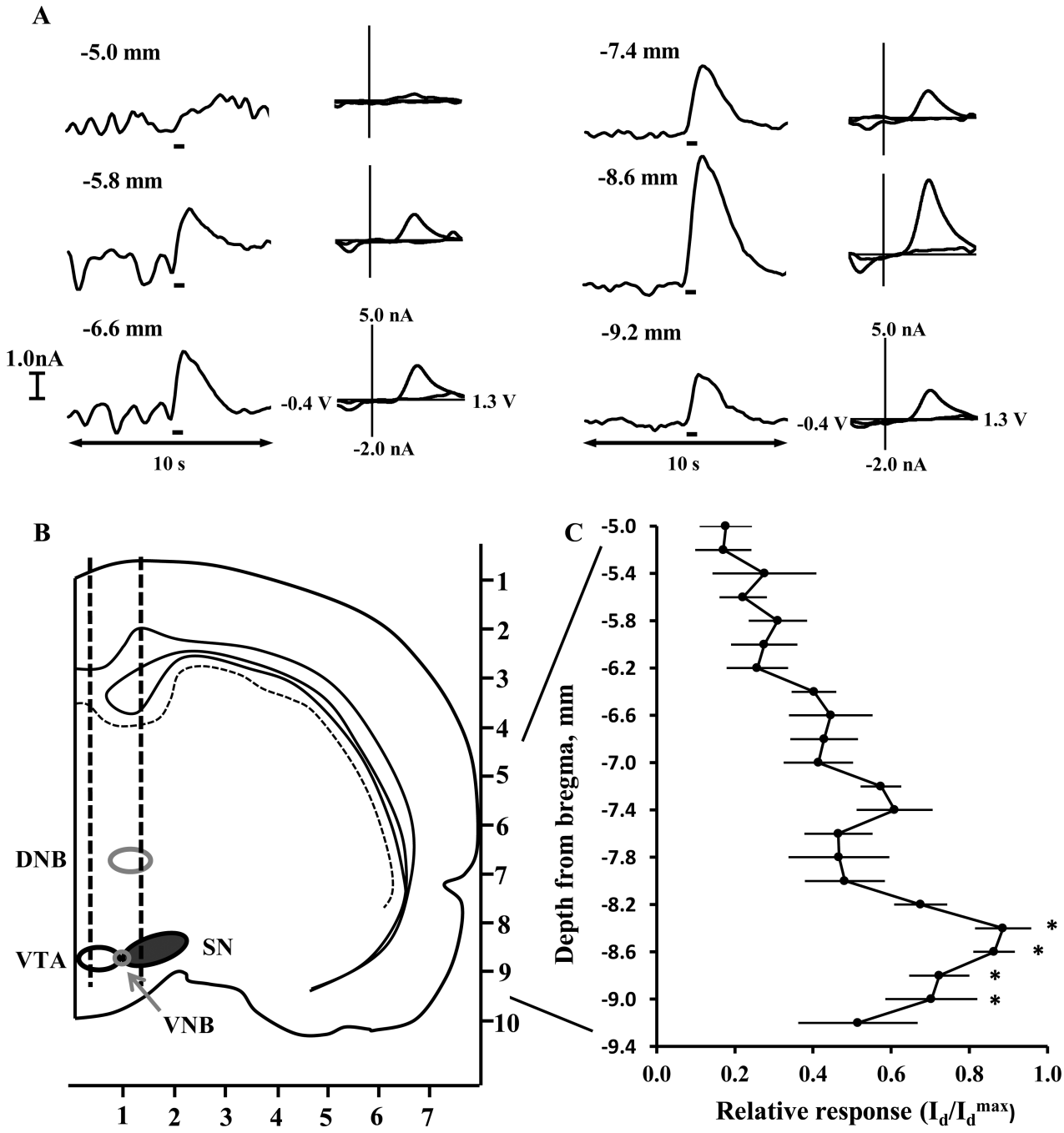

Figure 1.

CA transients in the mPFC of rats evoked by midbrain stimulation. (A) Representative current-versus-time traces and corresponding cyclic voltammograms detected in an individual rat. The current at the oxidation potential for CA is shown ±5s around the electrical stimulation (rectangle). The cyclic voltammogram indicates current at the full range of applied potentials measured at the peak of the CA release event. (B) The track of the bipolar stimulating electrode (dotted lines indicate the two wires) through the midbrain, axes in mm, adapted from (Paxinos and Watson, 1998). (C) Electrically-evoked CA release

in the mPFC presented as function of midbrain stimulation site (n=5 rats). The evoked CA signals (I_d) were normalized in each rat by dividing by maximal response observed in the rat (I_d^{max}). * significantly different from −5.0 mm depth, $p<0.05$. Abbreviations: DNB, dorsal noradrenergic bundle; SN, substantia nigra; VNB, ventral noradrenergic bundle; VTA, ventral tegmental area.

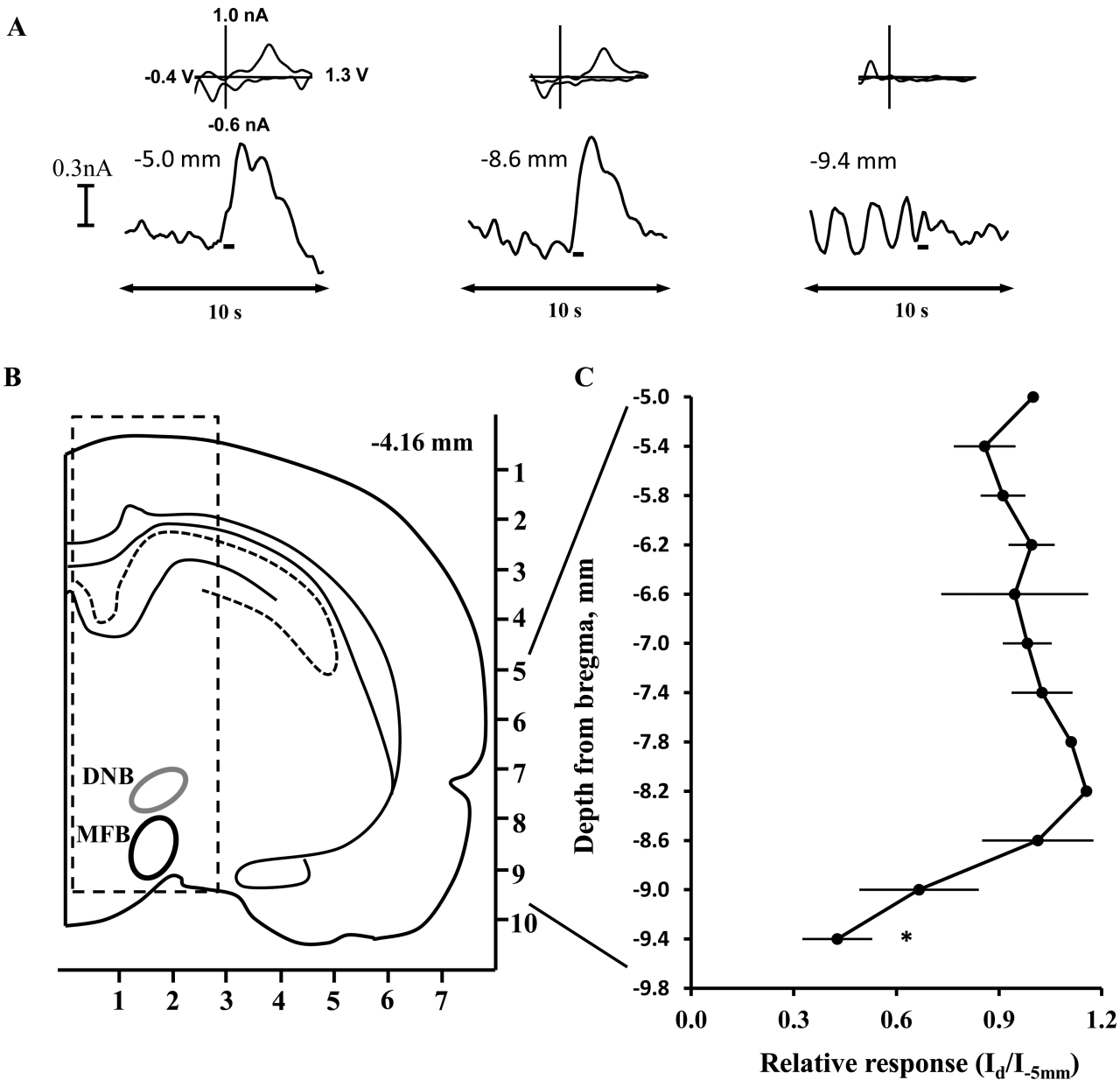

Figure 2.

VTA-evoked CA release in the mPFC before and after knife cut through the midbrain. (A) Representative current-versus-time traces and corresponding cyclic voltammograms detected in an individual rat. The current at the oxidation potential for CA is shown ±5s around the electrical stimulation (rectangle). The cyclic voltammogram indicates current measured at the full range of applied potentials at the peak of the CA release event. (B) The track of the knife (dotted lines) through the midbrain, axes in mm, adapted from (Paxinos and Watson, 1998). Abbreviations: DNB, dorsal noradrenergic bundle; MFB, medial forebrain bundle. (C) Electrically-evoked CA release presented as function of knife depth (n=4 rats). The VTA-evoked CA signals (I_d) were normalized in each rat by dividing by the

response observed in the rat when the knife was initially positioned (I_{-5mm}). * significantly different from −5.0 mm depth, $p<0.05$.

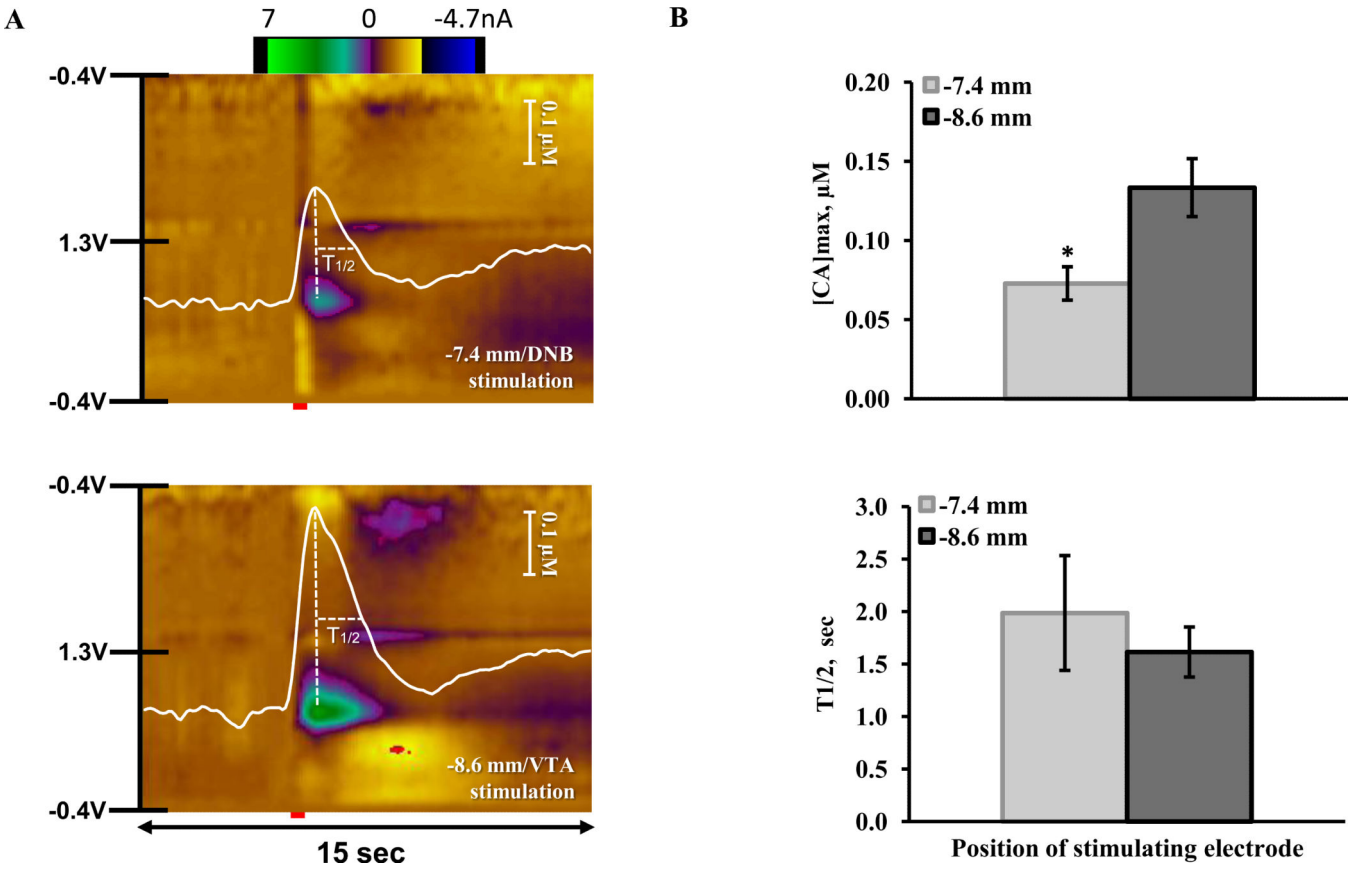

Figure 3.

Release and clearance of CA in the mPFC evoked by stimulation of the DNB and VTA. (A) Representative color plots of voltammetric signals detected in the mPFC of a single rat and evoked by midbrain stimulation (red rectangle) at −7.4mm (DNB, top) and −8.6mm (VTA, bottom) depth. The current at the oxidation potential of CA, converted to concentration, is overlaid on the color plot as a white line. The vertical dotted lines indicate the $[CA]_{max}$ of the electrically-evoked signals, and the horizontal dotted lines indicate the $T_{½}$. (B) $[CA]_{max}$ and $T_{½}$ obtained in the mPFC and evoked by electrical stimulation at the indicated depth (n=7 rats). * *p<0.05 versus −8.6mm stimulation.*

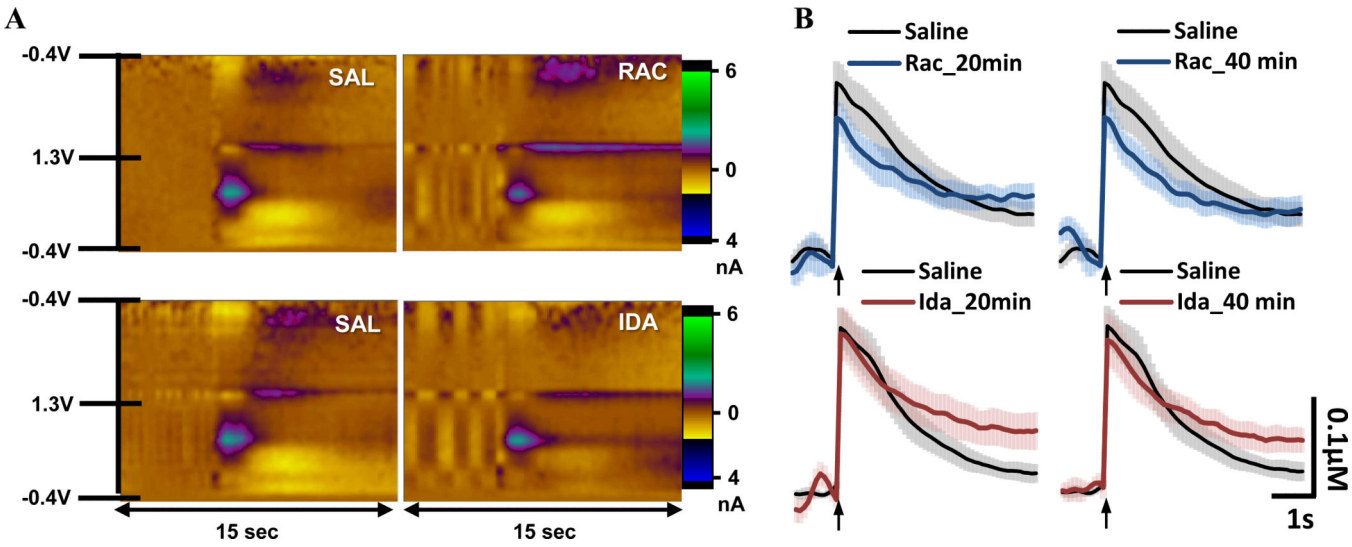

Figure 4.

Effects of D2 and α2-adrenergic receptor antagonists on VTA-evoked CA signals observed in the mPFC . (A) Color plots illustrate the electrically-evoked voltammetric signals obtained from individual rats and recorded after initial injections of saline and 20 min after subsequent injections of raclopride (RAC, top) and idazoxan (IDA, bottom). (B) [CA]-versus-time traces averaged from 6 rats demonstrate effect of RAC and IDA in 20 and 40 min after the injections (mean±SEM). The peaks of CA signals were aligned across rats.

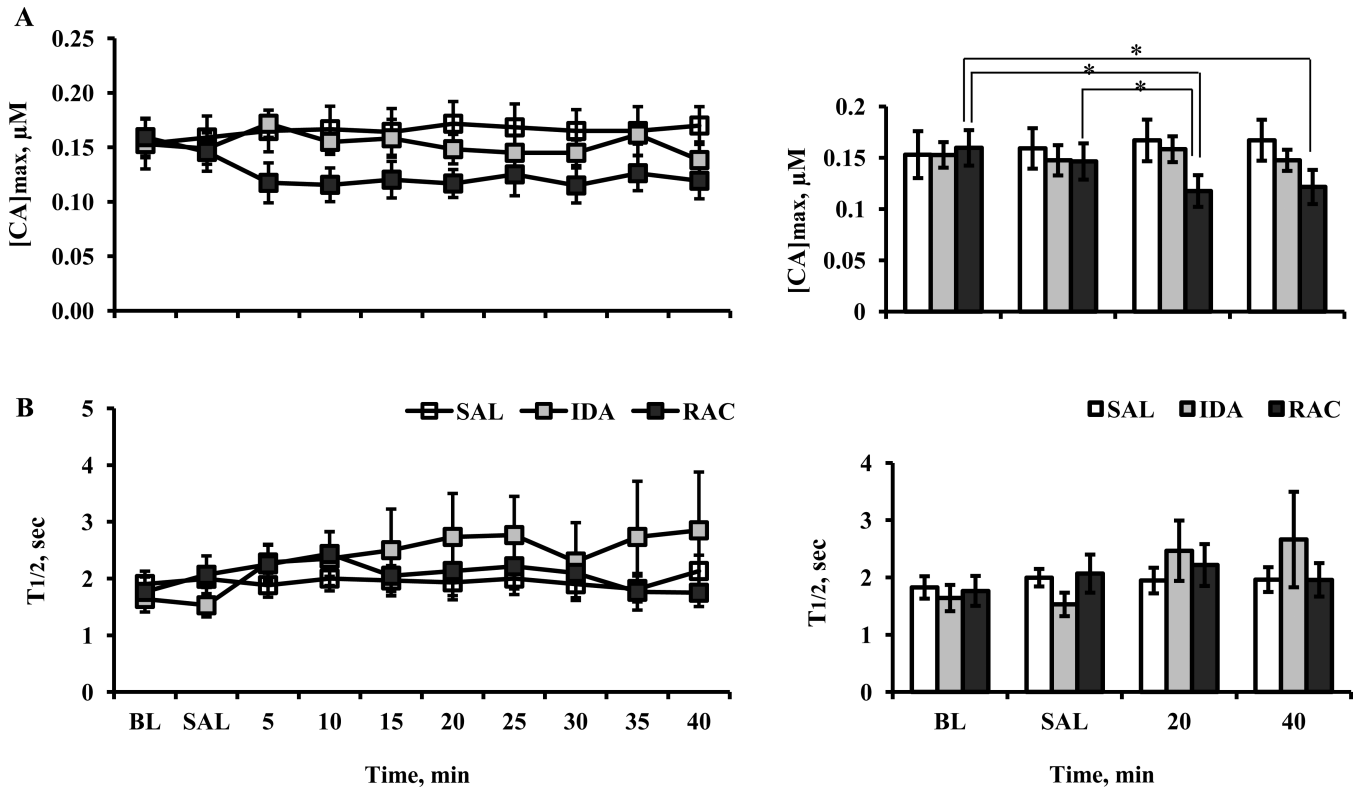

Figure 5.

Effects of D2 and α2-adrenergic receptor antagonists on (A) CA release and (B) clearance in the mPFC evoked by VTA stimulation. Left: $[CA]_{max}$ and $T_{1/2}$ over time; baseline (BL) and saline (SAL) time points are averaged from 4 samples each, followed by individual time points after drug administration at time 0 (SAL, saline; IDA, idazoxan; RAC, raclopride). Right: Data from the left panels are collapsed across time into 20-min epochs; n=6/group. **comparisons significantly different, $p<0.05$.*